GLOBAL JOURNAL OF PURE AND APPLIED SCIENCES, VOL.7, NO. 4, SEPTEMBER 2001: 695-705
 ISSN 1118-0579

LABORATORY MEASUREMENT AND INVERSION OF THE 2-DIMENSIONAL GEOELECTRIC RESPONSE OF A HYDROCARBON-IMPACTED SAND FORMATION

M. O. OLORUNFEMI, A. I. OLAYINKA, and F. O. AKINLUYI

(Received 28 December 2000; Revision accepted 13 March, 2001)

ABSTRACT

The environmental impact of oil spills is a major issue and problem in Nigeria presently, especially in the oil-producing communities. As part of a programme to test the application of geophysics as a non-invasive subsurface waste location technique, we have employed laboratory and computer modelling techniques to investigate the usefulness of two-dimensional (2-D) geo-electrical imaging in providing a better understanding of the problem.

A simulated oil spill tank has been carefully constructed in the Department of Geology, Obafemi Awolowo University, Ile-Ife, and designed to resemble an oil spill as closely as possible. The tank was made of plank and strong enough to withstand the pressure of the sandfill. The interior wall was lined with polythene to prevent seepage of the saturating fluid. The tank was filled with well-sieved river valley sand, saturated with water and the resistivity of the sand taken, this serving as control. The sand was then contaminated with crude oil and the 2-D apparent resistivity pseudosection data measured. A wall effect test, involving pole-pole array, was carried out in order to determine the area within which geoelectric measurements could be taken without significant wall effect.

Five electrical traverse lines were established in the tank. Measurements were made with the Wener, pole-pole, and pole-dipole arrays for electrode spacings 2, 4 and 6 cm along the 5 traverses. In addition, dipole-dipole data were measured for 5 levels of the pseudosection along one of the traverses. The dipole-dipole data were inverted using a Simultaneous Iterative Reconstruction Technique (SIRT) algorithm.

The apparent resistivity maps show that, with any of the four arrays used, the hydrocarbon-impacted sand is identified as a high apparent-resistivity anomaly. Inversion of the dipole-dipole data indicates that while the limits of the spill can be accurately defined, its depth extent may be slightly overestimated.

In this paper, the usefulness of 2-D geoelectrical imaging as a tool for mapping oil spills has been demonstrated and this has significance for environmental impact assessment in the Niger Delta hydrocarbon province.

KEY WORDS: environmental impact, oil spill, inversion, resistivity anomaly.

INTRODUCTION

The environmental impact of oil spills is a major issue and problem in Nigeria presently, especially in the oil-producing communities. Oil spills can occur due to a variety of reasons (Ozumba et. al., 1999), including operators' errors, equipment failure, corrosion of pipelines, sabotage (notably pipeline vandalisation), workover fluids spillage, pigging operations, dredging, flowline replacements, flowstation upgrades, tank rehabilitation, and natural phenomena such as heavy rainfall, flooding, falling trees and lightning (Table 1). It has been estimated that the Nigerian National Petroleum Corporation (NNPC) has some 21 000 km of pipelines. The oil spills have far-reaching effects on human, livestock, vegetation, forestry and wildlife, aquatic life, land use, soil and agriculture, climate and air quality. Undoubtedly, oil pollution is one of the environmental challenges facing the society at large. After an oil spill had occurred it is often desirable to determine the spatial and depth extent of the pollution. This investigation may involve direct drilling or the use of non-invasive methods such as remote sensing, geobotany, aerial photography and geophysics. It has been shown that carefully designed geophysical investigations

M. O. OLORUNFEMI, Department of Geology, Obafemi Awolowo University, Ile-Ife, Nigeria
A. I. OLAYINKA, Department of Geology, University of Ibadan, Ibadan, Nigeria
F. O. AKINLUYI, Departement of Geology, Obafemi Awolowo University, Ile-Ife, Nigeria

Table 1. Causes and components of oil spills in the Niger Delta (adapted from Dimkpa et al., 1997; Kragha and Adepoju, 1994; Okara et al., 1998; Ozumba, 1998; Ozumba, 1999; Ozumba et al., 1999)

Cause	Component(s)
Production	
- (subsurface conditions)	Blow-out due to overpressure during drilling and production
- (human error)	Operators'/Maintenance technicians errors
- (equipment error)	Equipment failures e.g. seals failures
Corrosion	Internal, external, erosion, sandcut of pipelines, fittings, etc
Sabotage/Theft	Vandalisation of oil production facilities e.g. flowlines, delivery lines, manifolds; Tampering (cutting and removal) of gaslift lines.
Miscellaneous	
- Drilling operations	Work-over fluids spillage, pigging operations.
- Engineering activities	Dredging, flowline replacements, flowstation upgrades, tank rehabilitation),
- Natural phenomena	Heavy rainfall, flooding, falling trees, lightning

can be employed to characterize hydrocarbon spill sites (Sauck et. al., 1998; Atekwana et. al., 2000). There are two main reasons for the use of geophysical methods to investigate environmental problems particulary hydrocarbon spillage. Firstly, geophysical methods can be employed to evaluate the extent of existing problems, predict where pollutants will go in the subsurface, and guide exploratory drilling programmes. Secondly, geophysical methods can be used prior to construction to help assess subsurface integrity at critical locations such as chemical plants, flow stations and waste storage disposal. The geophysical methods currently used in solving environmental problems include magnetic, seismic, ground penetrating radar, electromagnetic and electrical resistivity.

The principal aim of the present work is to investigate the usefulness of two-dimensional (2-D) electrical imaging as a non-invasive geophysical technique as part of an integrated environmental impact assessment (EIA). An experimental approach was adopted in which a tank was constructed, filled with well-sieved sand and the apparent resistivity measured, the data from this set-up serving as the control. Measurements were made with the Wenner, pole-pole, pole-dipole and dipole-dipole arrays. The sand body was then contaminated with crude oil, and the apparent resistivity re-measured. A qualitative impression of the effect of the crude oil was obtained by comparing the respective apparent resistivity maps for the pre-impacted and the post-impacted sand formation. The quantitative effect of crude oil contamination was, also, examined by inverting the respective sets of apparent resistivities. The specific objectives of the work are to: (i). generate characteristic geoelectrical signatures or pattern for the different electrode arrays over the unimpacted and the hydrocarbon-impacted sand formation, (ii). evaluate the sensitivity of the electrode arrays to the hydrocarbon impacted zone and, (iii). determine which electrode array (or combination of arrays) resolve(s) the hydrocarbon-impacted zone better both spatially and vertically.

METHOD OF STUDY

Laboratory scale modelling is often required in areas of complex geology and limited geophysical and geological control in order to generate responses typical of real field situations in the laboratory. It is used primarily to develop better understanding of geophysical responses from similar geologic setting, provide basis for an optimum exploration strategy and as an aid in interpretation.

A simulated oil spill tank (Fig. 1) was

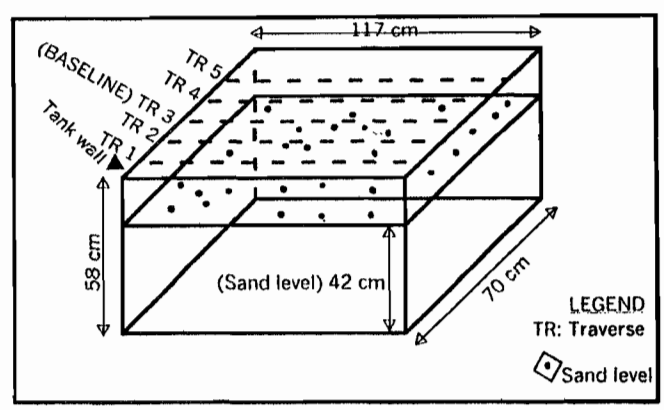

Fig. 1. Laboratory model tank showing measurement traverses.

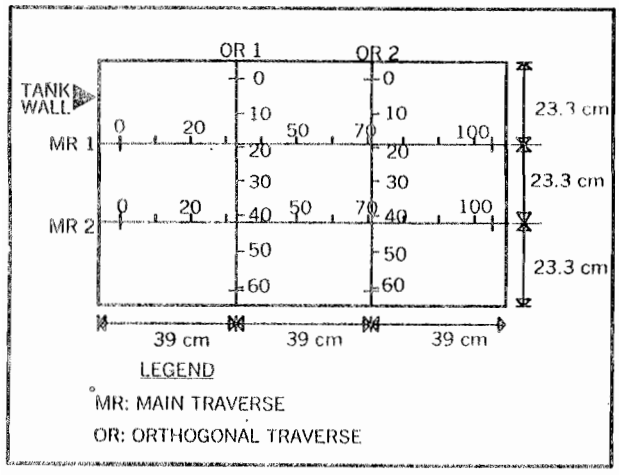

Fig. 2. Traverse layout for test for wall effect. The short ticks inside the tank represent measurement points along the respective traverses. The station separation is 2 cm.

carefully constructed in the Department of Geology, Obafemi Awolowo University, Ile-Ife, (Akinluyi, 2000) and designed to resemble an oil spill as closely as possible. The model tank was made of plank, strong enough to withstand the pressure of the sand fill. The tank is 117 cm long, 70 cm wide and 58 cm deep. The tank was filled with river valley sand, which was sieved in order to reduce lateral inhomogeneity. The tank was subsequently saturated with tap water. The interior wall was lined with polythene to prevent seepage of saturating fluid. A wooden board perforated at every 1 cm interval was used as electrode platforms for horizontal profiling measurements. A digital ABEM SAS 300C Terrameter resistivity meter was used for resistance measurements; these readings were subsequently converted into apparent resistivities by multiplying with the appropriate geometric factor. Three stages of measurements were carried out namely wall effect test, pre-hydrocarbon impact measurement and post-hydrocarbon impact measurement.

The model tank, being made of very resistive plank, could be expected to influence the apparent resistivity response of its immediate surroundings. In order to determine the area within the tank whose apparent resistivity response would be least influenced by the resistive wall of the tank, a wall effect test was carried out. This involved running resistivity profiles, with the pole-pole array, along two main traverses (MR1 and 2) and two orthogonal traverses (OR 1 and 2) (Fig. 2). The interelectrode spacing and station interval was 2 cm. The pole-pole resistivity profiles show near-uniform apparent resistivity values along the main and orthogonal traverses. Local highs were due to lateral inhomogeneity or wall effect. As would be expected, relatively high resistivity values were recorded near the tank walls due to the infinite resistivity of the wooden tank frame. The wall effect is noticeable within less than 5 cm of the tank wall. Subsequent resistivity measurements were, therefore, limited to the central 80 cm along the respective traverses (Fig. 3); in other words, the region 0 to 18.5 cm on either side of the tank wall was excluded from the measurements.

To serve as control, pre-impact resistivity profiles with Wenner, pole-dipole and pole-pole data were acquired for electrode spacings of 2 cm, 4 cm and 6 cm along all the five traverses. In addition, dipole-dipole measurements for $n=1$ to $n=5$ with an electrode spacing of 2 cm were made along line 3. The position and orientation of the traverses are shown in Fig. 3.

The central portion of the sand (25 cm x 25 cm) was impacted with crude oil (hydrocarbon) and left for about 24 hours to attain equilibrium. Due to the high permeability of the sand, the hydrocarbon spreadout attained an elliptical shape at the surface (Fig. 4). The resistivity measurements carried out on the unimpacted sand were repeated for the hydrocarbon-impacted sand. The same electrode arrays and spacing parameters were utilized.

As part of the data quality control, the following precautions were made: (i). the upper segment of the copper wire electrodes was rubber insulated so as to minimise the electrode contact resistance with the resistive wooden platform, (ii). electrodes were planted firmly on the sand in order to avoid error due to soil contact effect, (iii). measurements were taken as fast as possible to avoid resistivity

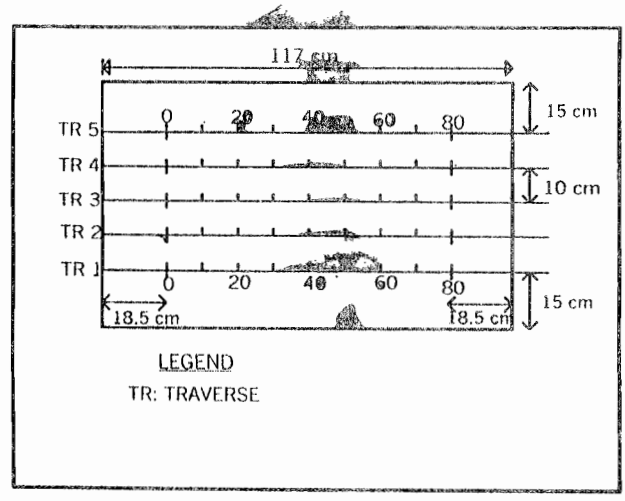

Fig. 3. Traverse layout for the pre-impact sand formation.

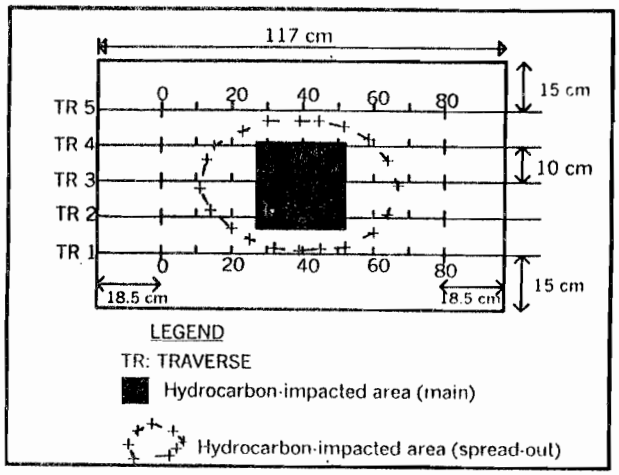

Fig. 4. Plan map of model tank showing hydrocarbon-impacted zone.

variations due to evaporation, (iv). instruments and cables were checked regularly to avoid malfunctioning and leakages. Apparent resistivity maps for the respective electrode spacings were prepared, these aimed at providing a semi-quantitative idea of the resistivity distribution with depth within the sand formation.

The dipole-dipole data were inverted using a Simultaneous Iterative Reconstruction Technique (SIRT).

INVERSION PROCEDURES

Automatic inversion procedures are often required in the reconstruction of the 2-D resistivity distribution. Most of the schemes work iteratively. The program, 2DSIRT by Weller et. al. (1996), was employed in the present work. It uses a finite difference approach to solve for the potential distribution due to point sources of current, and the potential distribution is converted into apparent resistivity values. The modelling routine accounts for 3-D sources (current electrodes) in a 2-D material model. This implies that the resistivity can vary arbitrarily along the line of surveying (x-direction) and with depth (z-direction), but the models have an infinite perpendicular extension along the strike (y-direction).

The steps involved are as follows (Olayinka and Weller, 1997):

(1) The subsurface is subdivided into blocks of constant resistivity. The number of blocks N is equal to the number of model parameters. All parameters may be described by a parameter vector $\mathbf{x} = (x_1, \ldots\ldots, x_n)^T$. The parameter x_j is defined as the logarithm of the resistivity of the jth block.

(2) The measured data are compiled in a data vector $\hat{\mathbf{y}} = (y_1, \ldots\ldots, y_M)^T$ where M corresponds to the number of measurements. The element y_i of the data vector y is the logarithm of the apparent resistivity of the ith measurement in the survey.

(3). A starting model is chosen. The parameter vector is initialized $\mathbf{x} = \mathbf{x}^{(0)}$

(4) The forward modelling for the model $\mathbf{x}^{(k)}$ is performed where k denotes the number of the model. The apparent resistivity is calculated for all M configurations of electrodes used in the field survey. The calculated data are compiled in a data vector y(k). The forward modelling is described by an operator S which is applied to the parameter vector x(k):

$$\mathbf{y}^{(k)} = S(\mathbf{x}^{(k)}). \qquad (1)$$

(5) The residual $\mathbf{r}^{(k)}$ between measured and computed data is determined:

$$\mathbf{r}^{(k)} = \mathbf{y}-\mathbf{y}(k) \qquad (2)$$

If a norm of the residual $||\mathbf{r}^{(k)}||$ is less than a predetermined value ε the iteration process can be stopped. The last model is accepted as a solution of the inversion.

(6) If the residual fails the stopping criterium the differences are applied to correct the resistivity model according to the inversion scheme and the next iteration is started with the forward modelling in step (4).

RESULTS AND DISCUSSION

The apparent resistivity maps for electrode spacings a = 2, 4 and 6 cm, for the Wenner array are presented in Fig. 5. It can be observed that the crude oil is identified as an apparent resistivity high at the three spacings. Moreover, the effect of the crude is not noticeable for traverses 1 and 5, indicating absence of contamination along these two lines. Similar results were obtained for the pole-dipole (Fig. 6) and the pole-pole arrays (Fig. 7).

In order to obtain some semi-quantitative idea of the sensitivity of the various electrode arrays used in the tank model experiment in identifying the resistivity anomaly, an anomaly

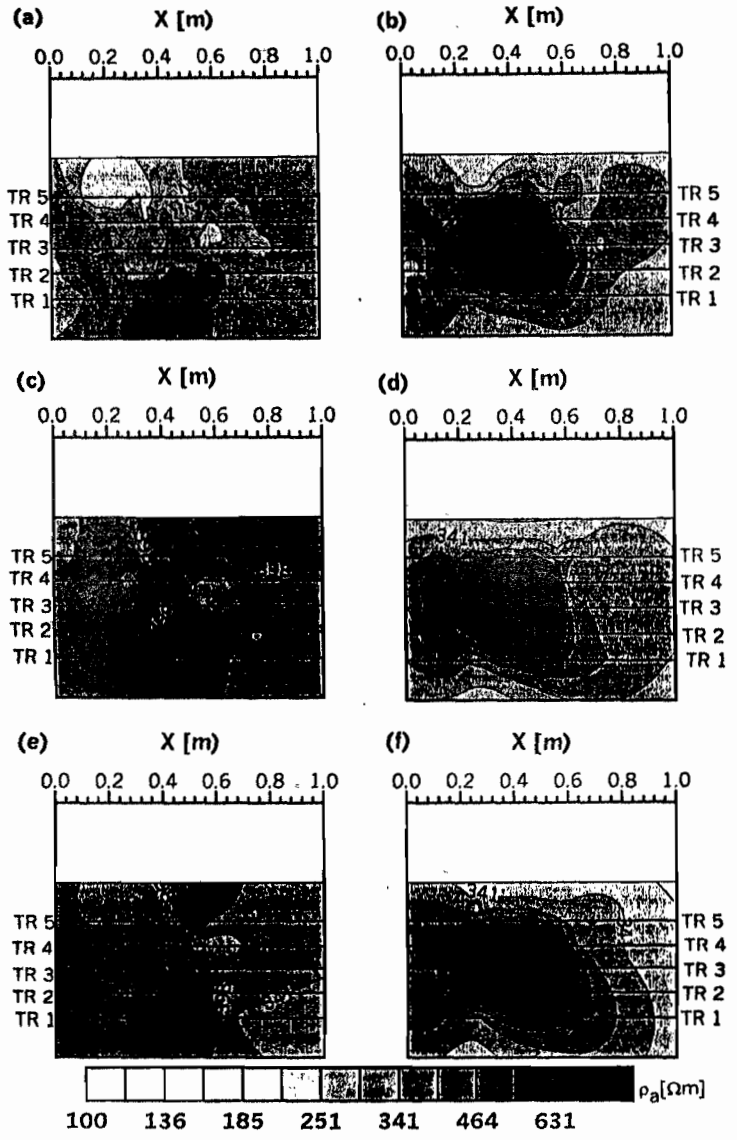

Fig. 5. Apparent resistivity maps for the Wenner array. (a) and (b), a= 2cm. (c) and (d), a= 4 cm. (e) and (f), a= 6 cm. The left hand panels are data for the pre-impact sand formation while the right hand panels are the correponding data for the post-impact sand.

index was adopted; this is defined simply as:

Anomaly index = post-impact ρ_a /pre-impact ρ_a

for the respective electrode spacings where ρ_a is the apparent resistivity. The higher the anomaly index the greater the ease with which the hydrocarbon contamination would be identified. The results for the spacings a = 2, 4 and 6 cm, for the pole-pole, pole-dipole and Wenner are shown in Fig.8. The response in the case of the pole-pole is, for all practical purposes, flat at about 1.48. That for the pole-dipole array is not much different. However, the Wenner shows a minimum at a = 4 cm.

The anomaly index for line 3 for all the four arrays is presented in Fig. 9. In comparison to Fig. 8, it can be observed that the anomaly index for this traverse, which is at the core of the crude-oil impact, is consistently greater than that for the entire tank, for each electrode spacing. This is consistent with the observation above that the crude oil contamination is largely restricted to traverses 2 to 4, with minimal effect on traverses 1 and 5 which are towards the outer parts of the tank.

The apparent resistivity pseudosection data measured along Traverse 3, which was at the centre of the tank, for the pre-impact sand is presented in Fig. 10a. The readings are generally very low, at between 246 and 1195 Ωm, with a mean of 574±170 Ωm, without any anomalous zone recorded. The corresponding pseudosection for the impacted sand (Fig. 10b) indicates a high resistivity

anomaly towards the centre of the tank. The resistivities vary between 256 and 3351 Ωm, with a mean of 1135±674 Ωm. The residual apparent resistivities (post-impact minus pre-impact) are shown in Fig. 10c. It can be observed that most of the values are positive, this being a reflection of higher resistivities from the crude oil. This, as should be expected, is in agreement with the ratio of the post-impact apparent resistivity to the pre-impact apparent resistivity (Fig. 10d) which varies between 0.6222 to 4.5050 with a mean of 2.0373±0.9361. The large deviations in the residuals can be attributed to heterogeneity of the sand formation.

The inversion results are presented in Fig. 11. There are some spurious anomalies at a depth of about 0.075 m for the pre-impact sand and these may be due to artefacts. The model resistivities for the pre-impact sand vary between 266 and 1414 Ωm, with a mean of 642±303Ωm. The data rms misfit (D_{rms}) is fairly high at 18% (Fig. 11a). There is a high resistivity anomaly for the resistivity image of the post-impact sand (Fig. 11b); its model resistivities vary between 318 and 5137 Ωm, with a mean of 1240±908 Ωm. The D_{rms} is slightly lower than that for the pre-impact sand at 15%. It has been shown that in the smooth inversion of apparent resistivity data, the D_{rms}

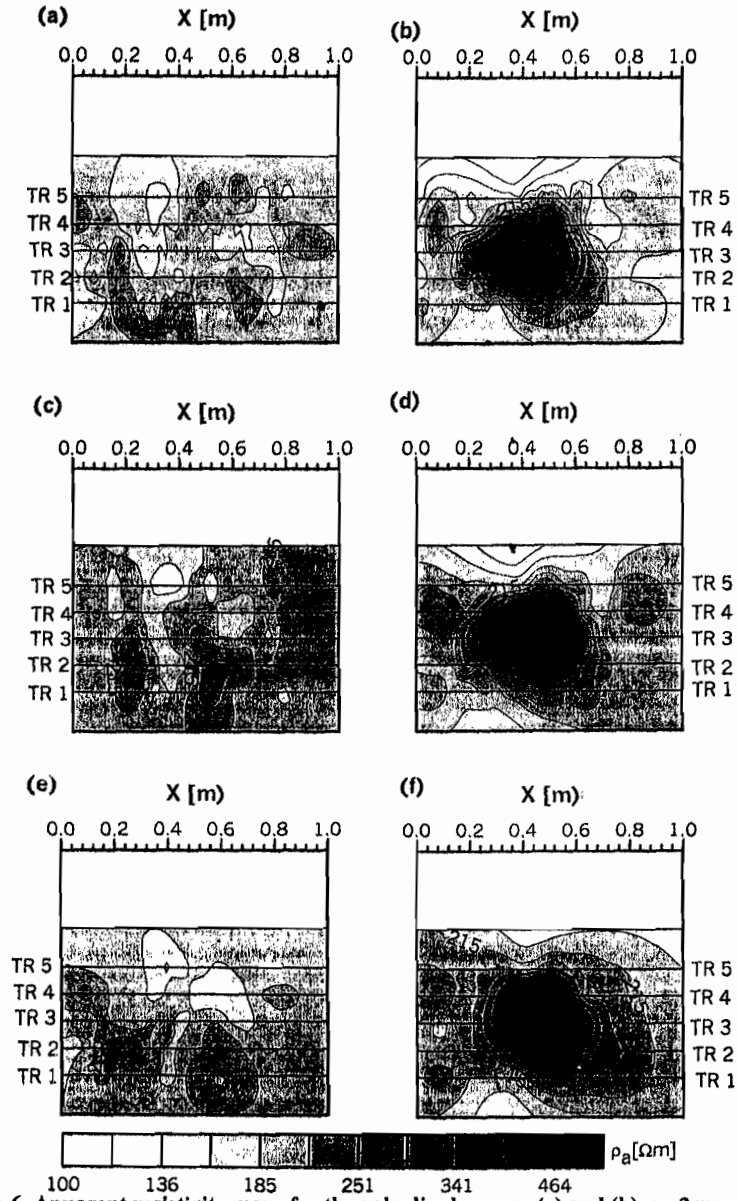

Fig. 6. Apparent resistivity maps for the pole-dipole array. (a) and (b), a= 2cm. (c) and (d), a= 4 cm. (e) and (f), a= 6 cm. The left hand panels are data for the pre-impact sand formation while the right hand panels are the corresponding data for the post-impact sand.

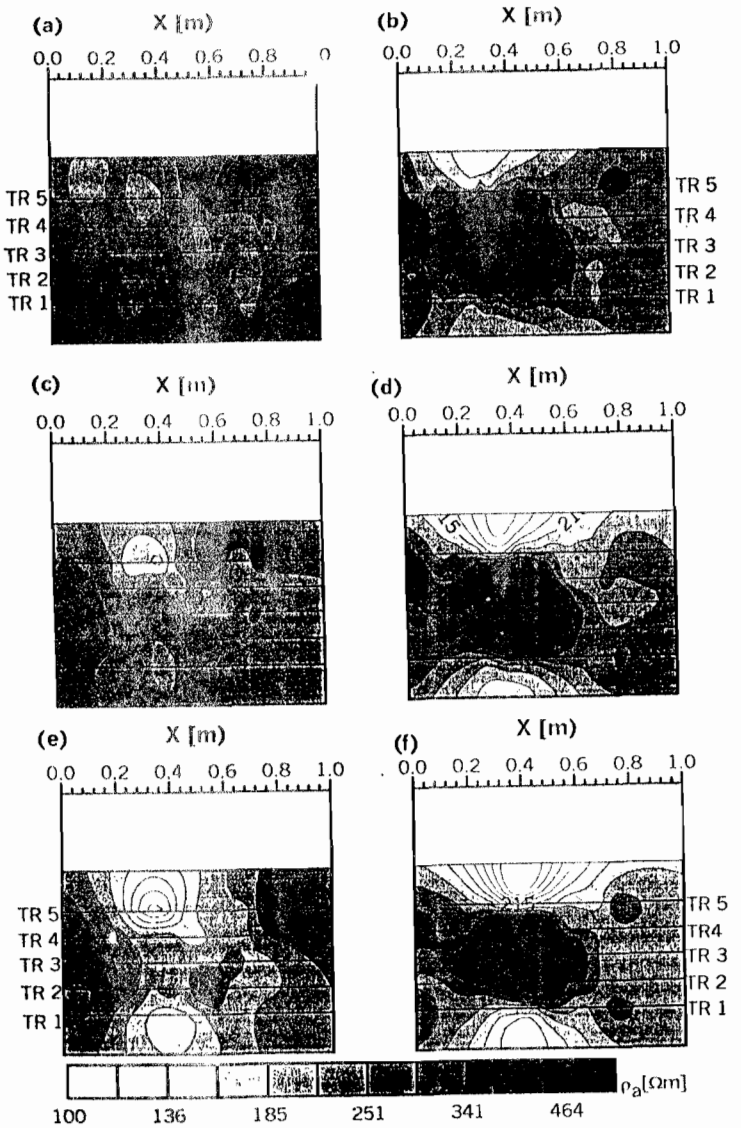

Fig. 7. Apparent resistivity maps for the pole-pole array. (a) and (b), a= 2cm. (c) and (d), a= 4 cm. (e) and (f), a= 6 cm. The left hand panels are data for the pre-impact sand formation while the right hand panels are the corresponding data for the post-impact sand.

tends to converge to the level of the noise in the data (Olayinka and Yaramanci, 2000a,b). This suggests that introduction of hydrocarbon (for the post-impact sand) has not led to an increase in the noise level; in its stead, there was a slight drop. The residuals between the post-impact and the pre-impact sands ranges between −472 and 4179 Ωm, with a mean of 598±761 Ωm (Fig. 11c) the large residuals may be partly due to heterogeneity of the sand as well as edge effects on the model (Beard and Morgan, 1991; Oldenburg and Li, 1999). Similarly, the ratio of the model resistivities in the impacted sand to the unimpacted sand is largely greater than one, varying between 0.4855 to 5.8993 with a mean of 1.8979±0.8892 (Fig. 11d).

The apparent resistivity data calculated from the resistivity models in Fig. 11a and b are presented in Figs 12a and 12 c, respectively. The corresponding data misfits are shown in Figs. 12b and 12d. The misfit space sections, especially that for the post-impact sand, indicate that there is a large underestimation of the apparent resistivities (with negative values of data misfit) at the shallowest level of the pseudosection. It was very difficult to reduce this during modelling as there is an overestimation of apparent resistivities at larger electrode spacings. These are also reflected in the large standard deviations of the misfits.

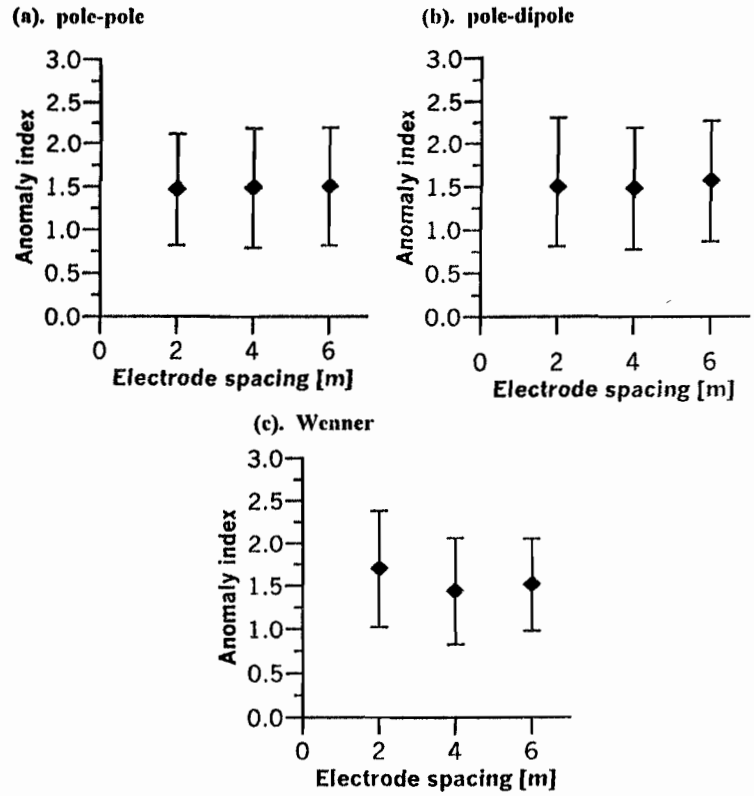

Fig. 8. Ratio of apparent resistivity measured for the post-impact sand to that for the pre-impact sand at the respective electrode spacings as a way of defining the anomaly index. The indices have been calculated for all the data points in the pseudosection in each case. The bars are in terms of the mean ± standard deviation.

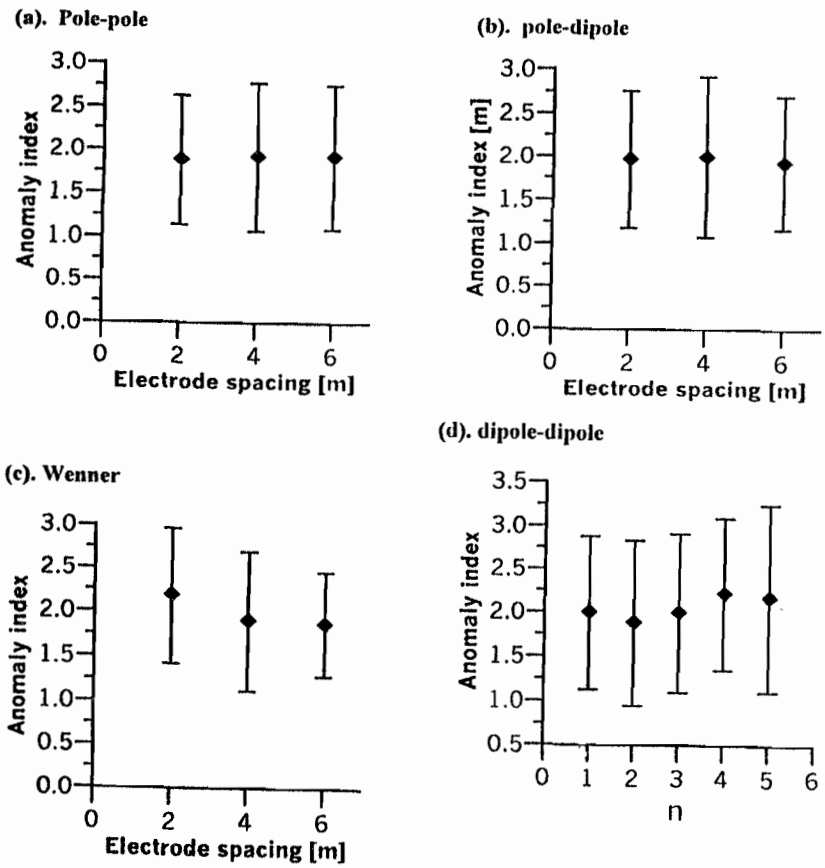

Fig. 9. Comparison of the anomaly index along Line 3 for the respective electrode arrays.

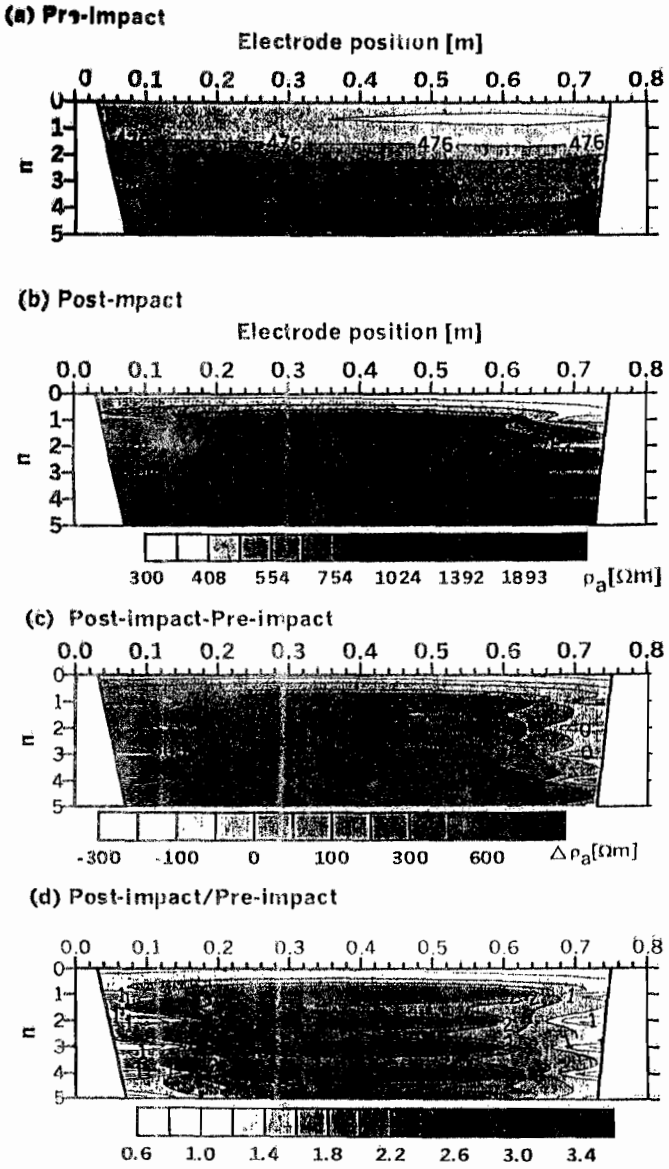

Fig. 10. Measured dipole-dipole apparent resistivity pseudosection data alongTraverse 3. (a). Pre-impact sand. (b). Post-impact sand. (c). Residual apparent Resistivities (post-impact minus pre-impact). (d). Ratio of Post-impact/Pre-impact.

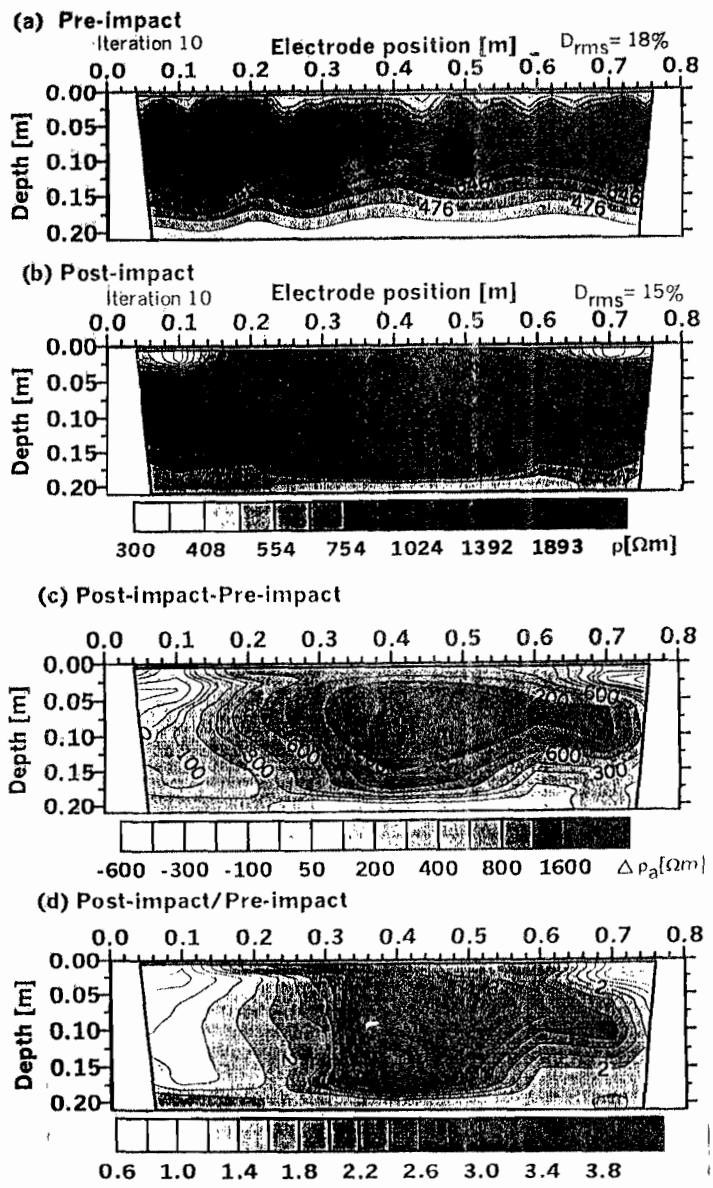

Fig. 11. Inversion results of the data alongTraverse 3. (a). Pre-impact sand. (b). Post-impact sand. (c). Residual apparent resistivities (post-impact minu pre-impact). (d). Ratio of Post-impact/Pre-impact.

A starting model, comprising three geoelectrical units having a decrease in resistivity with depth, and a sharp boundary between the layers, shown in Fig. 13a, was employed in interpreting the measured data. The pseudosection data calculated from this model is presented in Fig. 13b and the data rms misfit is very high at 62%, suggesting a poor fit. After trial and error adjustment to this model, the model in Fig. 13c was obtained, with a substantial reduction in the data rms misfit to 28%. The corresponding pseudosection data is shown in Fig. 13d. Our experience with modelling and inversion of resistivity data over 2-D structures has shown that the data misfit tends to be larger when constraints are imposed on the inversion process such as by specifying the starting model by the interpreter (Olayinka and Yaramanci, 2000c).

CONCLUSIONS

In this paper, a non-invasive geophysical technique, based on electrical tomography has been applied to determine the lateral and depth extent of a simulated oil spill. The results indicate that the hydrocarbon-impacted sand is identified as a high resistivity anomaly. The anomaly is readily identified on any of the four electrode arrays used for measurement,

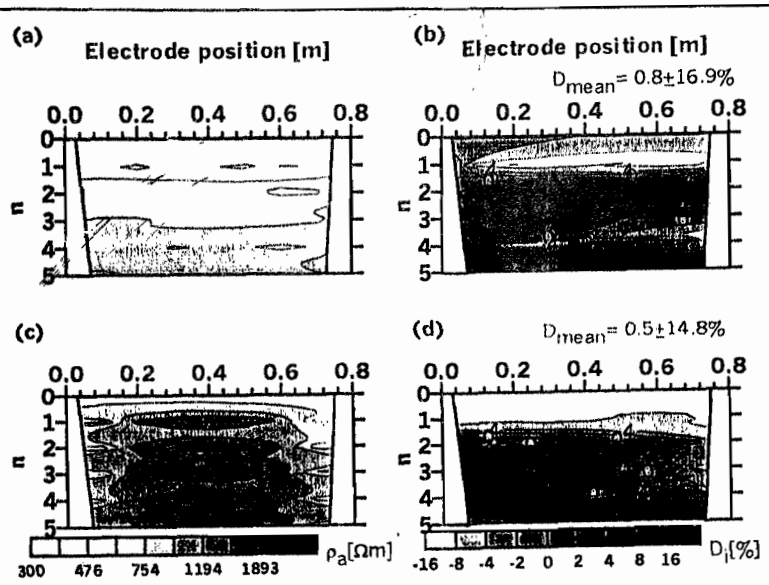

Fig. 12. Calculated apparent resistivity data (left hand panel) and the corresponding data model resistivity space section (right hand panel) from the electrical images in Fig. 11a and b.

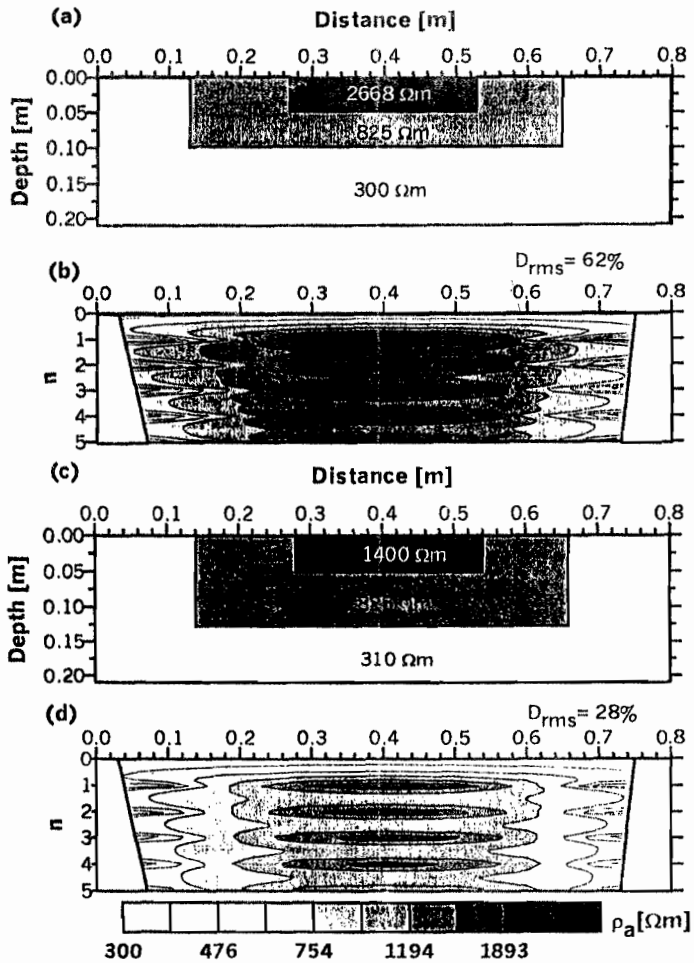

Fig. 13. 2-D resistivity image for the post-impact sand formation. (a) starting 2-D model (b). pseudosection data calculated from the model in (a). (c). 2-D model after 10 iterations. (d). pseudosection data calculated from the model in (c).

indicating the suitability of these electrode configurations for this type of investigation. Inversion of the dipole-dipole data along the central traverse indicates that while the limits of the spill can be accurately defined, its depth extent may be slightly overestimated.

This paper has demonstrated the usefulness of 2-D geoelectrical imaging as a

tool for mapping oil spills and has significance for environmental impact assessment in the Niger Delta hydrocarbon province. Our further work is aimed at 3-D data collection and inversion.

ACKNOWLEDGEMENT

This paper was first presented during the 18th Annual International Conference of the Nigerian Association of Petroleum Explorationists, in Abuja, November 2000. AIO is grateful to the Postgraduate School, University of Ibadan, for the funding provided.

REFERENCES

Akinluyi, F.O., 2000. Laboratory modelling of geoelectric response of hydrocarbon impacted sand formation. MSc dissertation, Obafemi Awolowo University, Ile-Ife.

Atekwana, E.A., Sauck, W.A., and Werkema, D.D., 2000. Investigations of geoelectrical signatures at a hydrocarbon contaminated site. Journal of Applied Geophysics, 44, 167-180.

Beard, L.P. and Morgan, F.D., 1991. Assessment of 2-D resistivity structures using 1-D inversion. Geophysics, 56, 874-883.

Dimkpa, E.C.E., Adepoju, O.J. and Adefila, O.P., 1997. Environmental impact assessment (EIA) of the Escravos and Gbetiokun/Adagbassa Prospect areas. NAPE Bulletin, 12, No 1, 70-74.

Kragha, P.U. and Adepoju, P.J., 1994. Community problems and 3D seismic in the Niger Delta, SPDC experience. NAPE Bulletin, 9, No 1, 47-50.

Okara, I.C., Nwachukwu, J.A., Kutlay, S. and Olotu, S., 1998. Occupational health and environmental management in seismic operation. NAPE Bulletin, 13, No. 1, 31-36.

Olayinka, A.I. and Yaramanci, U., 2000a. Assessment of the reliabilty of 2D inversion of apparent resistivity data. Geophysical Prospecting, 48, 293-316.

Olayinka, A.I. and Yaramanci, U. 2000b. Inversion of 2-D pseudosection data in presence of a decrease in resistivity with depth. Proceedings of the 6th Meeting, Environmental and Engineering Geophysics Society- European Section, Bochum, Germany, 3 to 7. Sept 2000. Paper EL04, 4 pp.

Olayinka, A.I. and Yaramanci, U. 2000c. Use of block inversion in the 2-D interpretation of apparent resistivity data and its comparison with smooth inversion. Journal of Applied Geophysics, 45, 63-81.

Olayinka, A.I. and Weller, A., 1997. The inversion of geoelectrical data for hydrogeological applications in crystalline basement areas of Nigeria. Journal of Applied Geophysics, 37, 103-115.

Oldenburg, D.W. and Li, Y., 1999. Estimating depth of investigation in dc resistivity and IP surveys. Geophysics, 64, 403-416.

Ozumba, C.I., 1998. Corrosion and sabotage spills in SPDC (W) 1987-1996. NAPE Bulletin, 13, No 1, 37-49.

Ozumba, C.I., 1999. Oil spills and environmental impact – a case study of a sabotage incident in Foutorugbene. NAPE Bulletin, 14, No 1, 76-85.

Ozumba, C.I., Ozumba, M.B. and Obobaifo, C.E., 1999. Striking a balance between oil exploration and protecting the environment: The SPDC experience, NAPE Bulletin, 14, No 2, 130-135.

Sauck, W.A., Atekwana, E.A. and Nash, M.S., 1998. High conductivities associated with an LNAPL plume imaged by integrated geophysical techniques. Journal of Environmental and Engineering Geophysics, 2, No 3, 203-212.

Weller, A., Seichter, M., and Kampe, A., 1996. Induced-polarization modelling using complex electrical conductivities. Geophysical Journal International, 127, 387-398.